JACS
JOURNAL OF THE AMERICAN CHEMICAL SOCIETY
Communication
pubs.acs.org/JACS

Click and Patterned Functionalization of Graphene by Diels–Alder Reaction

Jing Li,[†,‡] Meng Li,[†] Li-Li Zhou,[‡] Shuang-Yan Lang,[†,‡] Hai-Yan Lu,[‡] Dong Wang,[*,†] Chuan-Feng Chen,[*,†] and Li-Jun Wan[*,†]

[†]Key Laboratory of Molecular Nanostructure and Nanotechnology and Beijing National Laboratory for Molecular Sciences, Institute of Chemistry, Chinese Academy of Sciences (CAS), Beijing 100190, P. R. China

[‡]University of CAS, Beijing 100049, P. R. China

Supporting Information

ABSTRACT: Chemical functionalization is a promising approach to controllably manipulate the characteristics of graphene. Here, we designed *cis*-dienes, featuring two dihydronaphthalene backbones, to decorate a graphene surface via Diels–Alder (DA) click reaction. The installation of a diene moiety into a nonplanar molecular structure to form *cis*-conformation enables a rapid (~5 min) DA reaction between graphene and diene groups. Patterned graphene of sub-micrometer resolution can be obtained by easily soaking poly(methyl methacrylate)-masked graphene in solution of hydroxyl-substituted *cis*-diene at room temperature. The functionalization degree can be further controlled by carrying out the reaction at higher temperature. The present result gives important insight into the effect of molecular conformation on the graphene functionalization process, and provides an effective and facile method for graphene functionalization.

As a two-dimensional (2D) atomic crystal composed of highly conjugated sp^2 carbon atoms, graphene exhibits excellent electrical, thermal, and mechanical properties[1] and has inspired a broad range of applications.[2] Chemical functionalization is one of the promising approaches[3] to controllably engineer the energy band structure,[4] create novel graphene derivatives,[5] and manipulate the interfacial characteristics of graphene.[3a] One of the greatest challenges for graphene chemical functionalization originates from its strong chemical inertness and stability; thus, highly reactive chemical radicals[3a,6] or harsh reaction conditions[3c] are generally needed. Cycloaddition, with the merits of no requirement of catalysts and simultaneous formation of a pair of sp^3 carbons,[7] is a class of reaction used to decorate graphene, taking advantage of the unsaturated and conjugated chemical structure of graphene. However, the unique 2D and giant conjugated structure of graphene make it have different and more chemically inert reactivity than the small molecules. Thus, a graphene functionalization reaction with high reactivity and mild reaction conditions is highly desired.

Diels–Alder (DA) reaction between a conjugated diene and a substituted alkene (dienephile) is an important class of synthetic reaction and is referred to as a "click-type" reaction due to its high efficiency, versatility, and selectivity. Haddon et al.[8] demonstrated that graphene could act as both diene and dienophile to react with representative dienophiles and dienes under certain conditions. Although the dienophile character of graphene is proven to be slightly stronger than its behavior as a diene,[9] the as-reported dienes have low DA reactivity with graphene at room temperature. Bian et al.[10] found that the DA reaction between cyclopentadiene and graphene could be triggered by mechanical force, which was utilized to achieve patterned functionalization of graphene. Zhu et al.[11] reported the inverse electron demand DA reaction of graphite using tetrazine derivatives at room temperature.[11]

Herein, we find that the *cis*- and *trans*-conformation dienes, which show a nondetectable difference in DA reactivity with small dienophile molecules,[12] have totally different DA reactivity on graphene film. The conformation of diene was fixed by installing it into two cyclic aromatic hydrocarbon backbones. The nonpolar structure of *cis*-diene can both maintain the favorable conformation for DA reaction and greatly decrease the strain effect during cycloaddition, thus resulting in "click-type" DA reaction between *cis*-diene and graphene at room temperature. Furthermore, we demonstrate that the DA reaction can achieve finely patterned functionality with the assistance of a poly(methyl methacrylate) (PMMA) mask. The degree of functionalization can be further controlled by carrying out the reaction at higher temperature. The DA reaction provides an effective, thermally stable method for functionalization of graphene, with improved electrically conductivity. Field-effect transistors (FETs) and Hall-effect measurements confirm that the DA reaction can have a p-type doping effect and improve graphene's conductivity.

The graphene used in this work is mainly chemical vapor deposition (CVD)-grown on a Cu substrate or transferred onto other supporting substrates.[13] The preferential conformations of **D1** and **D2** are *cis* and *trans*, respectively, after installation of a diene into two nonplanar backbones, dihydronaphthalene (**D1**) or indene (**D2**), as shown by the X-ray diffraction (XRD) results in Figure 1a. As revealed in Figure 1c, soaking the graphene/SiO_2 sample in **D1** solution for 5 min at room temperature can result in the presence of a D peak (~1350 cm^{-1}) in the Raman spectrum, which is related to the graphene defects and sp^3 C formation,[14,15] and a significant decrease of the double-resonance 2D peak (~2680 cm^{-1}). In contrast, no

Received: February 29, 2016
Published: June 6, 2016

DOI: 10.1021/jacs.6b02209
J. Am. Chem. Soc. 2016, 138, 7448–7451

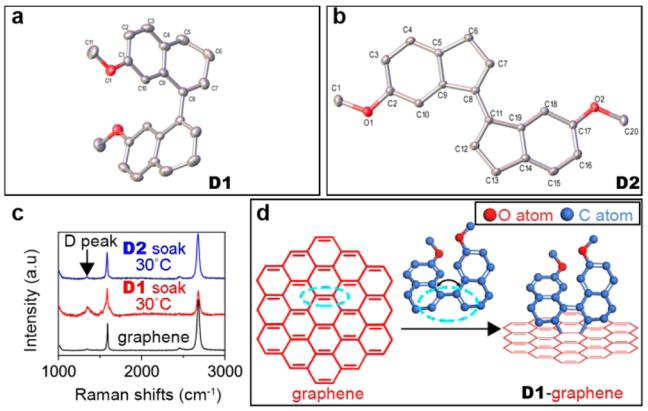

Figure 1. Crystal structures of (a) **D1** and (b) **D2** as characterized by XRD. (c) Raman spectra of graphene before and after soaking graphene/SiO_2 sample in **D1** and **D2** solution for 5 min at room temperature. (d) Schematic representation of the DA reaction between **D1** and graphene. The reaction site is highlighted by the dashed cyan circle. The hydrogen atoms are omitted for clarity in each molecular structure.

discernible Raman spectral changes were observed in control experiments with **D2** solution or pure solvents without **D1** molecules (Figures S1 and S2). Figure 1d illustrates the DA reaction scheme between **D1** and graphene.

The rapid DA reaction between **D1** and graphene, even at room temperature, promises a facile method to achieve patterned functionalization of graphene. The well-controlled functionalization pattern was achieved on graphene with the assistance of PMMA film as a mask, a technique which is widely used in CVD graphene transfer[16] and surface lithography.[17] The hydroxyl-substituted diene **D3** was designed and dissolved in isopropanol, which is not a solvent for the PMMA mask. The DA functionalization was conducted by simply soaking the patterned graphene/SiO_2 sample in **D3** solution for 10 min (Figure 2a). Graphene with a visible hexagon pattern was obtained by photolithography on PMMA film (Figure 2b). Raman D-peak intensity mapping (Figure 2d) reveals that the exposed region is effectively functionalized with **D3** molecules, while the PMMA-protected regions remain intact (Figure 2e). Atomic force microscopy (AFM) topography shows little height variation (Figure 2f,h) between the functionalized and nonfunctionalized regions, presumably due to the relatively low degree of reaction for room-temperature functionalization. However, the pattern boundaries can be clearly distinguished by scanning kelvin probe microscopy (SKPM) as shown in Figure 2g,h, and the functionalized regions shows lower surface potential (~100 meV) compared with the pristine graphene region,[18] which demonstrates the effective tune result of **D3** on the surface characteristics of graphene. The cross-sectional profile in Figure 2h shows the sharp pattern edge, which suggests the high-resolution (sub-micrometer) pattern could be achieved by DA functionalization.

To further increase the degree of DA functionalization, the DA reactions were conducted at different reaction temperatures, and the experiments were carried out by heating the graphene/SiO_2 sample on a hot plate at the designated temperature after drop-casting 10 μL of **D1** solution onto the graphene surface (Figure S2). The time evolution of I_D/I_G of graphene samples are shown in Figure 3a. Higher reaction temperature results in higher I_D/I_G, indicating larger reaction degree. The I_D/I_G ratio keeps increasing to reach the plateaus after 5 min and beyond. The kinetic analysis demonstrates that the DA reaction is a first-order reaction (Figure 3b and Figure S6), and the activation energy is about 13.57 kJ·mol^{-1}, as shown in Figure 3c, which demonstrates the DA reaction to be a low-energy-barrier reaction.

To exclude the influence of the CVD grain boundaries and defects on the graphene reactivity,[19] the DA reaction was conducted on both single-crystal CVD graphene and mechanically exfoliated graphene (MEG). The D peak of

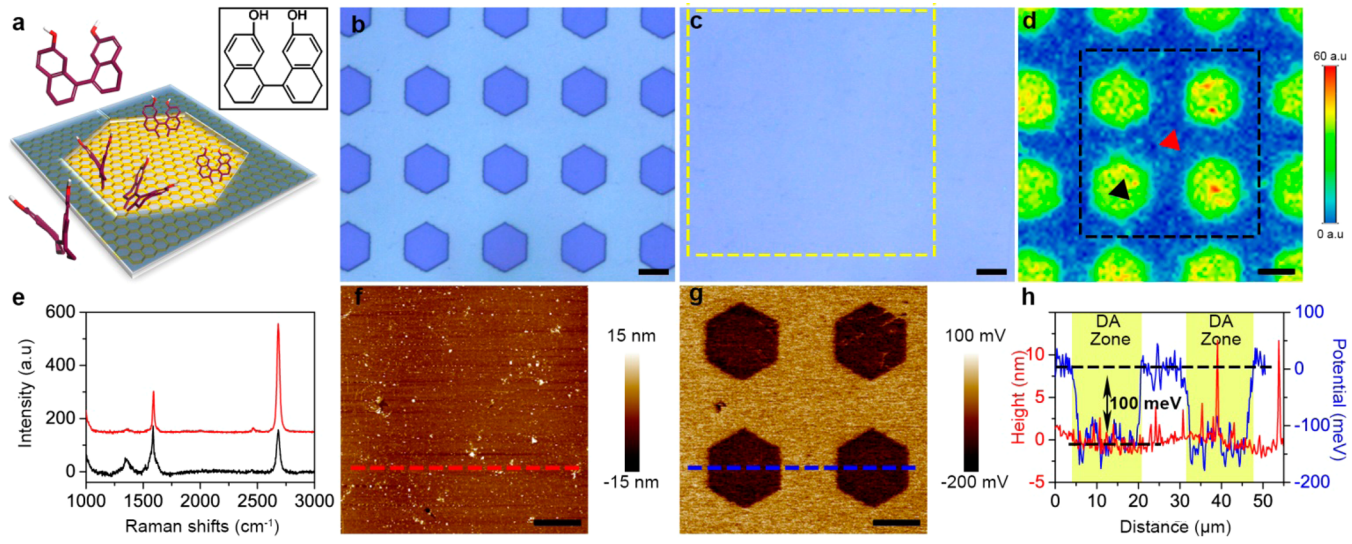

Figure 2. (a) Schematic of the procedure for patterned functionalization of graphene by **D3** (molecular structure as shown in inset) in isopropanol solution at room temperature. (b) Optical image of PMMA pattern on graphene. The dark blue hexagonal zones represent the exposure area of graphene. (c) Optical microscopy image of graphene surface after DA reaction and dissolving PMMA mask. (d) The D peak Raman mapping image of the graphene zone as marked by the yellow dashed rectangle in panel c. (e) Raman spectra of the graphene spots as marked by triangles in panel d. (f) AFM topography and (g) SKPM surface potential image of the graphene zone as marked by the black dashed rectangle in panel d. (h) Cross-sectional height (red line) and surface potential (blue line) profiles along the dashed line shown in panels f and g, respectively. The scale bars are 10 μm in each panel.

DOI: 10.1021/jacs.6b02209
J. Am. Chem. Soc. 2016, 138, 7448−7451

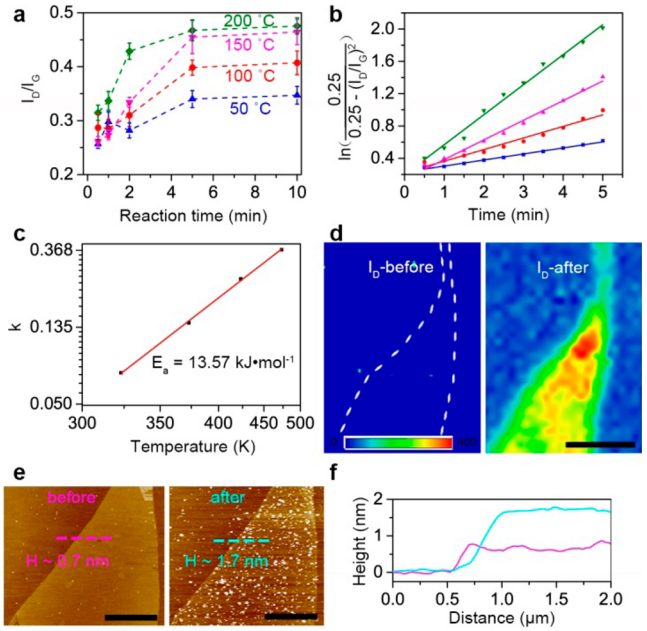

Figure 3. (a) Plot of Raman intensity ratios I_D/I_G of graphene as a function of time at different reaction temperatures. (b) Kinetic analysis of functionalization degree vs reaction time based on Raman data (see detailed kinetic derivation in SI). Solid lines are fitting curves on the basis of first-order kinetics. (c) Relationship between ln(k) and 1/T. The reaction rate constant k is derived from panel b. (d) D-peak Raman mapping of mechanically exfoliated graphene before and after DA reaction with **D1**. The scale bar is 10 μm. (e) AFM topological images of graphene before and after DA reaction. The scale bar is 2 μm. (f) Cross-sectional height profile along the dashed line in panel e.

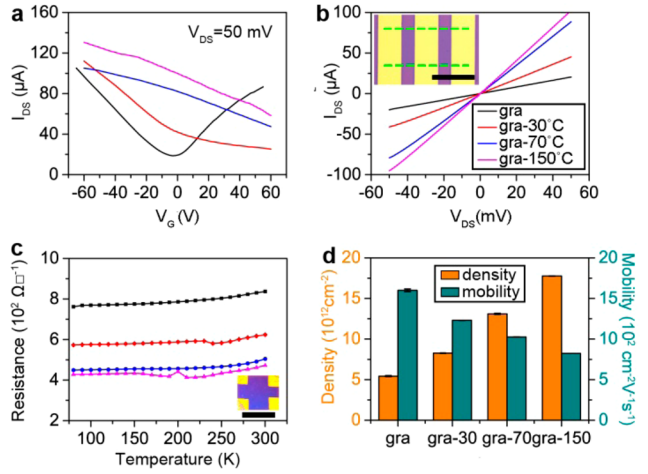

Figure 4. (a) I_{DS} versus V_G and (b) I_{DS} versus V_{DS} characteristics of the pristine graphene and the same graphene device which was consecutively reacted with **D1** at different temperatures. Inset in panel b: optical microscopy image of the FET device. The scale bar is 50 μm. The green dashed lines mark the graphene edges. The black, red, blue, and magenta lines represent pristine graphene and 30, 70, and 150 °C DA functionalized graphene, respectively, in panels a–c. (c) Electrical conductance change of pristine graphene sheet and the same graphene sample consecutively reacted with **D1** at different temperatures. Inset in panel c: optical microscopy image of the Hall bar device. The scale bar is 5 mm. (d) Histogram of carrier density and mobility in graphene and functionalized graphene as measured from the Hall bar devices.

Raman mapping intensity exhibits uniform distribution on the MEG surface (Figure 3d), which further confirms the homogeneous reactivity of the DA reaction. DA functionalization on thicker graphene is also feasible, as shown in Figure S8, and graphite can also be functionalized with *cis*-diene in 5 min at 200 °C. Additionally, the substrates underneath graphene show no influence on the graphene DA reactivity. It is worth mentioning that the **D1**-functionalized graphene demonstrates good thermal stability after annealing at 500 °C for 1 h (Figure S10).

Electrical transport measurements were performed to investigate the effect of DA functionalization on graphene's electrical properties. Graphene FETs were fabricated on 300 nm SiO_2/Si substrate with a top-contact, bottom-gate architecture. The pristine graphene exhibits an ambipolar character with a Dirac point around 0 V and carrier mobility between 1000 and 4000 cm^2 V^{-1} s^{-1}. Figure 4a shows that as the DA reaction degree increases, the Dirac point of graphene moves in the positive direction, demonstrating a p-type doping effect on graphene.[20] After 150 °C DA functionalization for 5 min, the carrier mobility is 500–1000 cm^2 V^{-1} s^{-1}. Figure 4b reveals the I–V character of the pristine and modified graphene. The slope of the I–V curve increases as the degree of DA functionalization on the graphene surface increases, which implies an improvement of conductivity.[21] To further elucidate the effect of DA functionalization on graphene's electrical properties, the Hall bar device was fabricated by shadow mask, as shown in Figure 4c. The resistivity of pristine graphene decrease from ~800 to 450 Ω/□ after functionalization, which is consistent with the FET results. As the extent of DA functionalization increases, the carrier mobility decreases gradually from ~1600 to ~800 cm^2 V^{-1} s^{-1} (Figure 4d). In contrast, the carrier density increases from 5 × 10^{12} to 1.7 × 10^{13} cm^{-2}. The covalently attached diene molecules on the graphene surface serve as electron-withdrawing groups to improve the hole density in graphene. Additionally, the hole-donating effect outweighs the mobility degradation effect, resulting in an improvement in the conductance of the graphene layer.

Although several covalent methods have been reported to modify graphene surfaces, most of them result in severe degradation of carrier mobility, thus limiting the further application of graphene in high-sensitivity sensor and electrical devices.[3b,4b,7] Diazonium salt is one of the most widely used chemicals to functionalize carbon nanotubes and graphene.[3a] A phenomenon similar to the graphene conductivity increase can be observed at a high extent of functionalization.[21] However, the coverage of diene molecules in this experiment is about 3% (quantitative analysis from the peak ratio of C 1s and Br 3d from the XPS measurement in Figure S5), which is lower than the typical result for diazonium chemistry (~12.5% coverage of nitrophenyl groups[3a]). The comparable improvement of conductivity at low coverage may be related to the simultaneous formation of a pair of sp^3 carbons caused by the DA reaction of one diene molecule.[7,22]

In summary, we demonstrate a simple, highly effective, and controllable Diels–Alder reaction to functionalize graphene by using *cis*-diene. The DA reaction can be finished in 5 min. The hydroxyl-substituted *cis*-diene molecule **D3** is compatible with the PMMA lithography process to realize patterned graphene by covalent functionalization. DA functionalization can have a p-type doping effect and cause an improvement in the conductivity of graphene films, which may be used as transparent electrodes.[23] The possibility to install other

DOI: 10.1021/jacs.6b02209
J. Am. Chem. Soc. 2016, 138, 7448–7451

functional groups on diene molecules through opposite benzene rings while maintaining the high DA reactivity makes *cis*-diene-based DA functionalization a promising way to achieve customized graphene derivatives for sensor applications. This click functionalization of graphene via DA reaction gives important insight into the effect of molecular conformation on the graphene functionalization process and provides an effective and facile method for graphene functionalization.

■ ASSOCIATED CONTENT

Supporting Information

The Supporting Information is available free of charge on the ACS Publications website at DOI: 10.1021/jacs.6b02209.

Experimental details and characterization data, and supplementary Figures S1−S11 (PDF)

■ AUTHOR INFORMATION

Corresponding Authors

*wangd@iccas.ac.cn
*cchen@iccas.ac.cn
*wanlijun@iccas.ac.cn

Notes

The authors declare no competing financial interest.

■ ACKNOWLEDGMENTS

This work was supported by National Natural Science Foundation of China (21127901, 21233010, 21433011, 21373236), and the Strategic Priority Research Program of the Chinese Academy of Sciences (Grant No. XDB12020100).

■ REFERENCES

(1) (a) Lee, C.; Wei, X.; Kysar, J. W.; Hone, J. *Science* **2008**, *321*, 385. (b) Novoselov, K. S.; Geim, A. K.; Morozov, S. V.; Jiang, D.; Zhang, Y.; Dubonos, S. V.; Grigorieva, I. V.; Firsov, A. A. *Science* **2004**, *306*, 666. (c) Chen, S.; Wu, Q.; Mishra, C.; Kang, J.; Zhang, H.; Cho, K.; Cai, W.; Balandin, A. A.; Ruoff, R. S. *Nat. Mater.* **2012**, *11*, 203.

(2) (a) Novoselov, K. S.; Falko, V. I.; Colombo, L.; Gellert, P. R.; Schwab, M. G.; Kim, K. *Nature* **2012**, *490*, 192. (b) Cao, X.; Yin, Z.; Zhang, H. *Energy Environ. Sci.* **2014**, *7*, 1850. (c) Yin, Z.; Zhu, J.; He, Q.; Cao, X.; Tan, C.; Chen, H.; Yan, Q.; Zhang, H. *Adv. Eng. Mater.* **2014**, *4*, 1300574.

(3) (a) Paulus, G. L. C.; Wang, Q. H.; Strano, M. S. *Acc. Chem. Res.* **2013**, *46*, 160. (b) Criado, A.; Melchionna, M.; Marchesan, S.; Prato, M. *Angew. Chem., Int. Ed.* **2015**, *54*, 10734. (c) Chua, C. K.; Pumera, M. *Chem. Soc. Rev.* **2013**, *42*, 3222.

(4) (a) Balog, R.; Jorgensen, B.; Nilsson, L.; Andersen, M.; Rienks, E.; Bianchi, M.; Fanetti, M.; Laegsgaard, E.; Baraldi, A.; Lizzit, S.; Sljivancanin, Z.; Besenbacher, F.; Hammer, B.; Pedersen, T. G.; Hofmann, P.; Hornekaer, L. *Nat. Mater.* **2010**, *9*, 315. (b) Bekyarova, E.; Sarkar, S.; Wang, F.; Itkis, M. E.; Kalinina, I.; Tian, X.; Haddon, R. C. *Acc. Chem. Res.* **2013**, *46*, 65.

(5) Wang, X.; Sun, G.; Routh, P.; Kim, D.-H.; Huang, W.; Chen, P. *Chem. Soc. Rev.* **2014**, *43*, 7067.

(6) Li, B.; Zhou, L.; Wu, D.; Peng, H.; Yan, K.; Zhou, Y.; Liu, Z. *ACS Nano* **2011**, *5*, 5957.

(7) Sarkar, S.; Bekyarova, E.; Haddon, R. C. *Mater. Today* **2012**, *15*, 276.

(8) (a) Sarkar, S.; Bekyarova, E.; Niyogi, S.; Haddon, R. C. *J. Am. Chem. Soc.* **2011**, *133*, 3324. (b) Cao, Y.; Osuna, S.; Liang, Y.; Haddon, R. C.; Houk, K. N. *J. Am. Chem. Soc.* **2013**, *135*, 17643.

(9) Denis, P. A. *Chem. - Eur. J.* **2013**, *19*, 15719.

(10) Bian, S.; Scott, A. M.; Cao, Y.; Liang, Y.; Osuna, S.; Houk, K. N.; Braunschweig, A. B. *J. Am. Chem. Soc.* **2013**, *135*, 9240.

(11) Zhu, J.; Hiltz, J.; Mezour, M. A.; Bernard-Gauthier, V.; Lennox, R. B.; Schirrmacher, R. *Chem. Mater.* **2014**, *26*, 5058.

(12) (a) Li, M.; Feng, L.-H.; Lu, H.-Y.; Wang, S.; Chen, C.-F. *Adv. Funct. Mater.* **2014**, *24*, 4405. (b) Li, Y.-Y.; Lu, H.-Y.; Li, M.; Li, X.-J.; Chen, C.-F. *J. Org. Chem.* **2014**, *79*, 2139.

(13) (a) Li, J.; Ji, H.; Zhang, X.; Wang, X.; Jin, Z.; Wang, D.; Wan, L.-J. *Chem. Commun.* **2014**, *50*, 11012. (b) Li, J.; Wang, X.-Y.; Liu, X.-R.; Jin, Z.; Wang, D.; Wan, L.-J. *J. Mater. Chem. C* **2015**, *3*, 3530.

(14) Ferrari, A. C.; Meyer, J. C.; Scardaci, V.; Casiraghi, C.; Lazzeri, M.; Mauri, F.; Piscanec, S.; Jiang, D.; Novoselov, K. S.; Roth, S.; Geim, A. K. *Phys. Rev. Lett.* **2006**, *97*, 187401.

(15) Kim, Y. A.; Fujisawa, K.; Muramatsu, H.; Hayashi, T.; Endo, M.; Fujimori, T.; Kaneko, K.; Terrones, M.; Behrends, J.; Eckmann, A.; Casiraghi, C.; Novoselov, K. S.; Saito, R.; Dresselhaus, M. S. *ACS Nano* **2012**, *6*, 6293.

(16) (a) Reina, A.; Jia, X.; Ho, J.; Nezich, D.; Son, H.; Bulovic, V.; Dresselhaus, M. S.; Kong, J. *Nano Lett.* **2009**, *9*, 30. (b) Li, X.; Cai, W.; An, J.; Kim, S.; Nah, J.; Yang, D.; Piner, R.; Velamakanni, A.; Jung, I.; Tutuc, E.; Banerjee, S. K.; Colombo, L.; Ruoff, R. S. *Science* **2009**, *324*, 1312.

(17) Xia, Y.; Rogers, J. A.; Paul, K. E.; Whitesides, G. M. *Chem. Rev.* **1999**, *99*, 1823.

(18) Xu, W.; Wang, L.; Liu, Y.; Thomas, S.; Seo, H.-K.; Kim, K.-I.; Kim, K. S.; Lee, T.-W. *Adv. Mater.* **2015**, *27*, 1619.

(19) (a) Cummings, A. W.; Duong, D. L.; Nguyen, V. L.; Van Tuan, D.; Kotakoski, J.; Barrios Vargas, J. E.; Lee, Y. H.; Roche, S. *Adv. Mater.* **2014**, *26*, 5079. (b) Wang, B.; Puzyrev, Y.; Pantelides, S. T. *Carbon* **2011**, *49*, 3983.

(20) Schedin, F.; Geim, A. K.; Morozov, S. V.; Hill, E. W.; Blake, P.; Katsnelson, M. I.; Novoselov, K. S. *Nat. Mater.* **2007**, *6*, 652.

(21) Huang, P.; Zhu, H.; Jing, L.; Zhao, Y.; Gao, X. *ACS Nano* **2011**, *5*, 7945.

(22) Sarkar, S.; Bekyarova, E.; Haddon, R. C. *Acc. Chem. Res.* **2012**, *45*, 673.

(23) Ryu, J.; Kim, Y.; Won, D.; Kim, N.; Park, J. S.; Lee, E.-K.; Cho, D.; Cho, S.-P.; Kim, S. J.; Ryu, G. H.; Shin, H.-A. S.; Lee, Z.; Hong, B. H.; Cho, S. *ACS Nano* **2014**, *8*, 950.

DOI: 10.1021/jacs.6b02209
J. Am. Chem. Soc. 2016, 138, 7448−7451